Energy Proceedings
Vol 57, 2025
ISSN 2004-2965

# A Statistical Characterization Method for the Migration of $CO_2$-Responsive Nanoparticle in Porous Media

Gang Huang[1,2], Bin Yuan [1,2*], Wei Zhang[1,2]

1 Laboratory of Unconventional Oil & Gas Development, China University of Petroleum (East China), Ministry of Education, Qingdao 266580, P. R. China

2 School of Petroleum Engineering, China University of Petroleum (East China), Qingdao 266580, P. R. China
(*Corresponding Author: yuanbin@upc.edu.cn)

**ABSTRACT**

$CO_2$-responsive nanoparticles are injected into the formation to enhance oil recovery by improving reservoir heterogeneity and increasing macro sweep efficiency. As the particles migrate within the pore space, their size increases with the rise in the pH of the aqueous phase. Consequently, particles cause plugging when the pH decreases. However, the lack of a suitable model for particle migration limits the optimization of particle injection. An easy-to-understand and effective description of the particle migration process is essential for making accurate predictions.

This research introduces a novel model for particle migration. First, a pore network model is used to represent the pore structure. Then, by considering changes in particle size due to pH and treating the total particle concentration as an independent variable, Markov chain theory is applied to develop quantitative relationships between the amount of plugged particles and the total number of particles. Finally, a new control model of particle migration is established, and a comparison between theoretical predictions and experimental results is provided to validate its accuracy.

**Keywords:** CCUS, $CO_2$-responsive nanoparticle, compositional simulation, Statistical characterization method

**NONMENCLATURE**

| | |
|---|---|
| *Abbreviations* | |
| CCUS | Carbon capture, utilization, and storage |
| $CO_2$-WAG | $CO_2$ water-alternating-gas injection |
| $CO_2$-EOR | $CO_2$-enhanced oil recovery |
| WD | Weibull distribution |
| PVD | Pore volume distribution |
| WMD | Weibull mixture distribution |
| *Symbols* | |
| $wd(x)$ | Weibull distribution function |
| $\eta_i$, $\tau_i$, $\lambda_i$ | The parameters of the $i$-th WD |
| $N_{wd}$ | The number of WDs used in the WMD |
| $pvd(r)$ | Pore volume distribution function |
| $V_r$ | The volume of a bulk rock, $m^3$ |
| $\phi$ | The porosity of a bulk rock |
| $r$ | The size of a capillary tube |
| $C_\phi$ | The compressibility coefficient, $Pa^{-1}$ |
| $P_0$ | The reference pressure, Pa |
| $P$ | The current Pressure, Pa |
| $r_s$ | The particle size, m |
| $c$ | The concentration of the particles with size $r_s$ in the rock |
| $\vartheta(r_s)$ | The probability that the rock captures the particle with size $r_s$ |
| $p(r_s/r)$ | The probability that one capillary tube of size $r$ captures the particles with size $r_s$ |
| $P_r^{r_s}$ | The probability that the captured particle exists in a tube of size r |
| $\gamma(r_s)$ | The probability that the particle is captured |
| $S^{n+1}$, $S^n$ | The probability that the particle is in a suspended state at the next moment and at the current time |
| $C^{n+1}$, $C^n$ | The probability that the particle is in a plugged state at the next moment and the current time |

# This is a paper for International CCUS Conference 2025 (ICCUSC 2025), May 28-29, 2025, Beijing, China.

| | |
|---|---|
| $S^0$, $C^0$ | The probability that the particle is in the suspended or plugged state at the initial time |
| $S^{final}$, $C^{final}$ | The probability that the particle is in the suspended or plugged state at the last time |
| $p_C$ | The possibility that the rock captures a particle |
| $\alpha$ | The shape factor of the injected particle |
| *Δpvd(r,0)* | After a particle is injected into a rock with no particles, the change in the pore volume of the capillary tubes with radius r |
| $\theta_1$ , $\theta_2$ , $\theta_3$ , $\theta_4$ | The parameters for the pore volume distribution model considering particle plugging |
| $\varepsilon_c$ | The critical concentration of particles that can exist in a rock |
| $\varepsilon_{pvd}$ | When *c* is increased to $\varepsilon_c$, the ratio of *pvd* to *pvd(r,0)* |
| *σ(c)* | The concentration of plugged particles with respect to the particle concentration *c* |
| $\chi(r_s/r_p)$ | The accessible coefficient describing the space that enables particles to occupy. |
| $\phi_p$ | The porosity considering the particle plugging |
| $\phi_a(r_s)$ | The accessible porosity is considered, considering the accessible coefficient for a particle |
| $v(r_s/r_p)$ | The flux reduction coefficient that describes the reduction of the flow ability due to the accessible characteristic of particles |
| $k_p$ | The permeability that considers the particle plugging |
| $k_a(r_s)$ | The accessible permeability that considers the flux reduction coefficient for a particle |
| $r_{s,max}$ | The maximum particle size, m |
| $\alpha$, $\beta$, $\gamma$ | The fitting parameters for the particle expansion model |
| $x_{CO2,w}$ | The $CO_2$ mole fraction in the aqueous phase |
| $K_{a1}$ | The first ionization constant of $CO_2$ in the aqueous phase |
| $S_o$, $S_g$, $S_w$ | The phase saturations of the oil, gas, and aqueous phases |
| $Ss$ | The saturation of the particle |
| $k_{ro}$, $k_{rg}$, $k_{rw}$ | The relative permeability without considering the influence of the particle. |
| $\rho_s$ | The concentration of particles in the aqueous phase |
| $\gamma_w$ | The gravity of the aqueous phase, Pa/s |
| $D$ | The depth, m |
| $q_w$ | The source or sink of the aqueous phase, $m^3/s$ |
| $c_s$ | The particle concentration in the source or sink, $mol/m^3$ |
| $\rho_j$ | The concentration of the j-th phase, $mol/m^3$ |
| $k_{rj}$ | The relative permeability of the j-th phase |
| $\mu_j$ | The viscosity of the j-th phase, Pa•s |
| $q_i$ | The source or sink of the i-th component, mol/s |
| $\rho_t$ | The total concentration of all components, $mol/m^3$ |
| $n_j$ | The phase mole fraction of the j-th phase |

## 1. INTRODUCTION

$CO_2$ water-alternating-gas injection ($CO_2$-WAG) has been proven to be an effective method for enhancing oil recovery (Abdullah and Hasan, 2021). Additionally, $CO_2$-WAG is also favorable for the $CO_2$ storage underground(Guo et al., 2022). However, the existence of high-permeability paths, such as high-permeability faults, fractures, or lens-shaped sand bodies, essentially increases the probability of gas channeling (Liu et al., 2019). To address this issue, nano-gel particle additives, such as $CO_2$-responsive nanoparticles, are being developed to achieve effective plugging of high-permeability channels (Deng et al., 2025). To decrease the risk of nanoparticle injection in the field and optimize the injection schedule, the reservoir-scale numerical simulation of the $CO_2$-responsive particle injection is indispensable. However, the lack of an effective macroscopic simulation to describe the particle blockage of the pore network during multiphase and multicomponent fluid flow limits the accuracy of optimizing $CO_2$-responsive particle flow. Consequently, there is an urgent need for a numerical simulation framework that considers key factors.

By incorporating $CO_2$-responsive functional groups, such as amidine groups, guanidine groups, and tertiary amino groups, into the molecular chain of the gel, the gel structure undergoes alteration in the presence of $CO_2$ (Cheng et al., 2024). Specifically, our attention is focused on those functional groups, exemplified by amidine groups, which can revert to their original state following a reduction in $CO_2$ concentration. Upon exposure to $CO_2$, the amidine group undergoes protonation, resulting in the formation of an amidine salt structure and the expansion of gel particles. During the expanding process involving $CO_2$ and $N_2$, the size of nanoparticles is observed to fluctuate within the range of 25 to 200 nm (Chen et al., 2023). Consequently, a transformation between the plugging and release states of nanoparticles can occur when the $CO_2$ concentration increases, as in the $CO_2$-enhanced oil recovery ($CO_2$-EOR) process. This unique characteristic of $CO_2$-responsive nanoparticles enables them to penetrate deeply into the reservoir, aggregate in high-permeability channels, and expand upon contact with $CO_2$, thereby forming blockages within these channels. Subsequently, the heterogeneity of the reservoir is mitigated, and the macroscopic sweep efficiency is augmented.

There are two primary methods of particle trap, the first is clogging, where the particle size is far away smaller than the pore size, particles attach the pore wall controlled by complicated surface force mechanism and reduce the pore size gradually; the second is plugging, where the particle has a counterpart size as the pore, particles plug the pore mechanically(Moghadasi et al., 2004; Cheng et al., 2024). By introducing the trapping rate and release rate, the behavior of $CO_2$-responsive nanoparticles can be theoretically implemented. Usually, $CO_2$-responsive nanoparticles are considered to have a size of 1-100nm, which leads to a significant mechanical plugging. Although the clogging of nanoparticles by accumulating in the pore space will occur, plugging is believed to be the dominant factor. It plays a leading role in sealing the high-permeability path. However, as nanoparticles, different from fines, the $CO_2$-responsive particles work mainly by mechanical plugging, which is usually a swift process. As a result, the characterization of the process of trapping and release by rate is assumed to have a similar prediction accuracy to that of characterization by a stable state. Moreover, describing the trapping and release of nanoparticles as an equilibrium process, the concentrations of trapped and suspended nanoparticles can be formulated as functions of the total particle concentration, which contributes to the construction of a reliable numerical simulation system.

Typically, the capillary bundle model is employed to characterize the probability of particle clogging, focusing on local physical processes and influenced by the local characteristics of the pore structure. Sharma and Yortsos (1987) calculated the probability that particles pass through a representative volume with a characteristic length using the product of several probability events, which includes the fluid velocity. Therefore, at least, the particle behavior within the pore space with a characteristic length should be described. The state of nanoparticles in the pore space can be either trapped or suspended; a probability controls the transformation between these two states. Markov chain theory is often used to describe the process of transitioning between different states. Considering the extensive pore microstructure and the frequent occurrence of the transition of particle state, a stable state of the Markov chain could provide a more representative value to estimate the probability of particle plugging.

This research proposes a novel particle migration model, in which the mechanical plugging of particles is considered the primary mode of plugging. Firstly, a pore network model is provided to depict the pore structure. Subsequently, the monotonic relationships among the quantities of plugged particles, suspended particles, and total particles are analyzed. After that, taking into account the variation in particle size due to pH and treating the amount of total particles as the independent variable, the Markov chain theory is utilized to formulate the quantitative relationships between the amounts of plugged particles and total particles, as well as the amounts of suspended particles and total particles. Next, based on the principle of volume balance, a model is constructed to characterize the alternation of pore structure caused by particle plugging, and the mathematical equations for porosity and permeability are derived. Eventually, a new control model of particle migration is established, and a comparison between theoretical predictions and experimental results is furnished to validate its accuracy. This new model provides an effective method for describing particle migration in relation to changes in particle size.

## *2. METHODS*

### *2.1 Particle transport model*

2.1.1 Pore structure model

The Weibull distribution (WD) is used to describe the variation in pore volume with the size of capillary tubes (pore volume distribution, PVD). Due to the complexity of the pore structure of the porous medium, a single WB can not describe the PVD of a porous medium exactly. Therefore, the Weibull mixture distribution (WMD), the linear combination of several WDs is applied to characterize the complicated PVD of a rock.

$$wd(x)=\sum_{i=1}^{i=N_{wd}}\eta_i\frac{\tau_i}{\lambda_i}\left(\frac{x}{\lambda_i}\right)^{\tau_i-1}e^{-\left(\frac{x}{\lambda_i}\right)^{\tau_i}}, \quad (1)$$

$$\sum_{i=1}^{i=N_{wd}}\eta_i=1, \quad (2)$$

where, $\eta_i$, $\tau_i$, $\lambda_i$ is the parameters of the *i*-th WD. Then the PVD can be expressed as,

$$pvd(r)=V_r\phi wd(r), \quad (3)$$

where $V_r$ is the volume of a bulk rock, $\phi$ is the porosity of a bulk rock, and *r* is the size of a capillary tube. Moreover, assuming that the capillary tube can be compressed exponentially, then the influence of pore pressure on the PVD is expressed as

$$pvd(r)=V_r\phi wd\left(\frac{r}{1+C_\phi(P-P_0)}\right)\left[1+C_\phi(P-P_0)\right]^2, \quad (4)$$

where $C_\phi$ is the compressibility coefficient, $Pa^{-1}$; $P_0$ is the reference pressure; *P* is the current pressure, Pa.

2.1.2 Particle plugging model

When particles are injected into a rock, they reach the balance of transport and plugging after a short time. Assume that the concentration of particles with a size of $r_s$ in the rock is *c*. Here, when a new particle is injected into the rock, the probability that the rock captures it can be expressed as

$$\vartheta(r_s)=\int_0^\infty p(r_s/r)wd(r)dr, \quad (5)$$

where, $\vartheta(r_s)$ is the probability that the rock captures the particle with size $r_s$; $p(r_s/r)$ is the probability that one capillary tube with size *r* captures the particles with size $r_s$. Obviously, the probability that one particle passes the next capillary tube is 1-$\vartheta(r_s)$.

During the transport of the particle in porous media, if the particle is captured, based on the definition of contingent probability, the probability that the captured particle exists in a tube with size *r* is expressed as,

$$P_r^{r_s}=\frac{p(r_s/r)wd(r)dr}{\vartheta(r_s)}. \quad (6)$$

Then, the particle is captured with a probability of

$$\gamma(r_s)=\int_0^\infty p(r_s/r)P_r^{r_s}=\int_0^\infty\frac{\left[p(r_s/r)\right]^2wd(r)dr}{\vartheta(r_s)}, \quad (7)$$

and released with a probability 1-$\gamma(r_s)$.

Before a particle passes a rock, it will flow through many capillary tubes. Therefore, it will be plugged sometimes and suspended at other times. To estimate the overall status of the particle, the Markov chain model is applied to calculate the average probability that a particle is captured or passes through a rock. For the two statuses of one particle, captured (C) and suspended (S) statuses, the transfer matrix is defined as follows,

$$\begin{bmatrix}S^{n+1}\\C^{n+1}\end{bmatrix}=\begin{bmatrix}1-\vartheta(r_s) & 1-\gamma(r_s)\\ \vartheta(r_s) & \gamma(r_s)\end{bmatrix}\begin{bmatrix}S^n\\C^n\end{bmatrix}, \quad (8)$$

*where $S^{n+1}$ and $C^{n+1}$ are the next possible statuses of the particle; $S^n$ and $C^n$ are the current possible statuses, as shown in Fig. 1.*

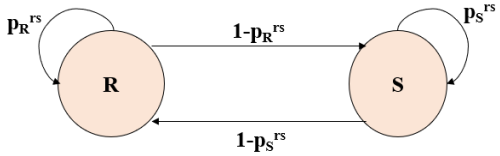


Fig. 1. The status transfer of the particle

Assuming that the initial status of the particle as

$$\begin{bmatrix}S^0\\C^0\end{bmatrix}=\begin{bmatrix}1\\0\end{bmatrix}, \quad (9)$$

the final status of the particle is calculated by,

$$\begin{bmatrix}S^{final}\\C^{final}\end{bmatrix}=\begin{bmatrix}1-\vartheta(r_s) & 1-\gamma(r_s)\\ \vartheta(r_s) & \gamma(r_s)\end{bmatrix}^{n\to\infty}\begin{bmatrix}1\\0\end{bmatrix}. \quad (10)$$

$$=\begin{bmatrix}\dfrac{1-\gamma(r_s)}{1+\vartheta(r_s)-\gamma(r_s)}\\ \dfrac{\vartheta(r_s)}{1+\vartheta(r_s)-\gamma(r_s)}\end{bmatrix}$$

The possibility that the rock captures a particle is calculated by

$$p_C = \frac{\vartheta(r_s)}{1+\vartheta(r_s)-\gamma(r_s)}. \quad (11)$$

After a particle is injected into a rock, the pore volume of the capillary tubes with radius *r* is reduced by

$$\Delta pvd(r,0) = -\alpha r_s^3 p_C(r_s) P_r^{r_s}, \quad (12)$$

where *α* is the shape factor of the injected particle. The derivative of pore volume of the capillary tubes with radius *r* with respect to particle concentration *c* is approximately calculated by

$$\begin{aligned} &\frac{dpvd(r,0)}{dc} \\ &= \left.\frac{\Delta pvd(r)}{\Delta c}\right|_{c=0,\Delta c\to 0} \\ &\approx -\alpha r_s^3 p_C(r_s) P_r^{r_s} \end{aligned}. \quad (13)$$

It is assumed that the change of pore volume with particle concentration satisfies the quadratic relationship, and the pore volume of the capillary tubes with size r can be expressed as

$$pvd(r,c) = \theta_1(r)c^2 + \theta_2(r)c + \theta_3(r). \quad (14)$$

At the same time, when c is increased to $\varepsilon_c$, the pvd is maintained at pvd(r,0)$\varepsilon_{pvd}$. Therefore,

$$pvd(r,c) = \begin{cases} \theta_1(r)c^2 + \theta_2(r)c + \theta_3(r); c < \varepsilon_c \\ pvd(r,0)\varepsilon_{pvd}; c \ge \varepsilon_c \end{cases}. \quad (15)$$

is provided. Besides, two implicit constraints are

$$pvd(r,0) = V_r \phi wd(r). \quad (16)$$

$$\left.\frac{\partial pvd(r,c)}{\partial c}\right|_{c=\varepsilon_c} = 0. \quad (17)$$

Based on Eqs. (13)-(17), $\theta_1$-$\theta_4$ can be calculated by

$$\theta_1 = \frac{\theta_2^2 - 2\theta_2}{4\left[pvd(r,0)\varepsilon_{pvd} - \theta_3\right]}, \quad (18)$$

$$\theta_2 = \alpha r_s^3 p_C(r_s) P_r^{r_s} c, \quad (19)$$

$$\theta_3 = V_r \phi wd(r), \quad (20)$$

$$\varepsilon_c = \frac{-\theta_2}{2\theta_1}. \quad (21)$$

The concentration of plugged particles is calculated by

$$\sigma(c) = \frac{pvd(r,0) - pvd(r,c)}{\alpha r_s^3}. \quad (22)$$

2.1.3 Petrophysical parameter

When the sizes of particles and pores are counterparts, the accessible coefficient is utilized to the space that enables particles to occupy, which is calculated as

$$\chi(r_s/r_p) = \begin{cases} 0, & r_s/r_p > 1 \\ (1 - r_s/r_p)^2, & r_s/r_p < 1 \end{cases}. \quad (23)$$

Then, based on the definition of the porosity, the porosity considering particles plugging and accessible porosity for particles are expressed as

$$\phi_p = \frac{1}{V_r \phi}\int_0^\infty V_p(r_p,c)dr_p, \quad (24)$$

$$\phi_a(r_s) = \frac{1}{V_r \phi}\int_0^\infty \chi(r_s/r_p) V_p(r_p,c)dr_p. \quad (25)$$

Similarly, the flux reduction coefficient is introduced to describe the reduction of the flow ability due to the accessible characteristic of particles, which is described mathematically as

$$v(r_s/r_p) = \begin{cases} 0, & r_s/r_p > 1 \\ (1 - r_s/r_p)^2\left[1 + 2r_s/r_p - (r_s/r_p)^2\right], & r_s/r_p < 1 \end{cases}, \quad (26)$$

Thus, assume that the flow is the Poiseuille flow, and based on the definition of permeability, the permeability considering particles plugging and accessible permeability for particles are written as

$$k_p = \frac{1}{V_r \phi}\int_0^\infty k_1(r_p) V_p(r_p,c)dr_p, \quad (27)$$

$$k_a(r_s) = \frac{1}{V_r \phi}\int_0^\infty k_1(r_p) v(r_s/r_p) V_p(r_p,c)dr_p. \quad (28)$$

*2.2 Particle/$CO_2$/oil/water multiphase flow simulation method*

2.2.1 Particle expansion model

Based on the data from the particle expansion experiments, the fitted mathematical model that describes the relationship between particle sizes and the mole fraction of $CO_2$ in the aqueous phase can be expressed as

$$r_s = \frac{r_{s,\max}}{1 + \gamma e^{\alpha\left[-\lg\left(\sqrt{0.001 x_{CO_2,w} K_{a1}} + 10^{-7}\right) - \beta\right]}}, \quad (29)$$

where, $r_{s,max}$ is the maximum particle size, m; *α*, *β*, *γ* are fitting parameters; $x_{CO2,w}$ is the $CO_2$ mole fraction in the aqueous phase; $K_{a1}$ is the first ionization constant of $CO_2$ in the aqueous phase.

2.2.2 Multiphase relative permeability model

The Particles are assumed to be completely encapsulated in the aqueous phase, which increases the

volume of the aqueous phase. As a result, considering the influence of particles on the volume of the aqueous phase, the new relative permeability model is written as

$$\begin{cases} k_{ro} = k_{ro}\left(S_o\right) \\ k_{rg} = k_{rg}\left(S_g\right) \\ k_{rw} = k_{rw}\left(S_w + S_s\right) \end{cases}, \tag{30}$$

where, $S_o$, $S_g$, $S_w$ are the phase saturations of the oil, gas, and aqueous phases; Ss is the saturation of the particle; $k_{ro}$, $k_{rg}$, $k_{rw}$ are the relative permeability without considering the influence of the particle.

$$\frac{\partial\left(\phi\sum_{j=1}^{j=n_p} S_j\rho_j x_{i,j}\right)}{\partial t} + \nabla\bullet\left[\sum_{j=1}^{j=n_p} x_{i,j}\rho_j \frac{k_{rj}k}{\mu_j}\left(\nabla p - \gamma_j \nabla D\right)\right], \tag{33}$$
$$+q_i = 0$$
$$i = 1,2,...,n_c;\quad j = o,g,w$$

where $\rho_j$ is the concentration of the j-th phase, mol/m$^3$;

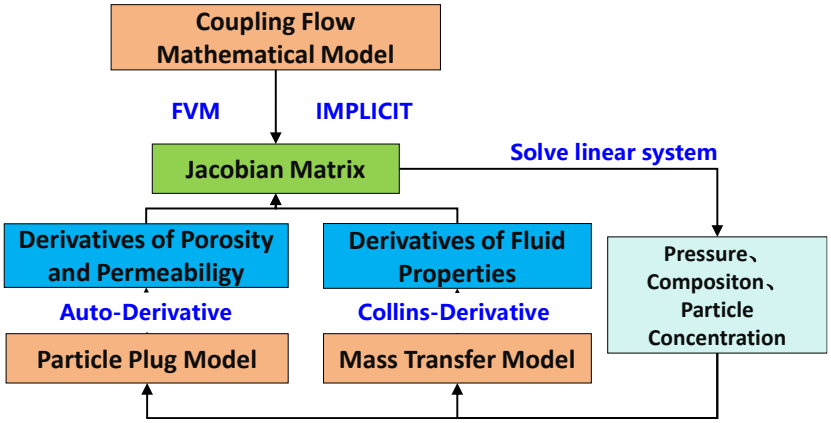


Fig. 2. The fully implicit solution method for the mathematical model for the particle/$CO_2$/oil/water multiphase flow.

2.2.3 Particle transport equation

The concentration of particles in the aqueous phase is calculated by combining the concentration of plugged particles and the accessible porosity as

$$\rho_s = \frac{c - \sigma}{\phi_a\left(S_w + S_s\right)}. \tag{31}$$

The control equation of particle transport is expressed as

$$\frac{\partial c}{\partial t} + \nabla\bullet\left[\rho_s \frac{k_{rw}k_a}{\mu_w}\left(\nabla p - \gamma_w \nabla D\right)\right] + q_w \bullet c_s = 0, \tag{32}$$

where, $\gamma_w$ is the gravity of the aqueous phase, Pa/s; $D$ is the depth, m; $q_w$ is the source or sink of the aqueous phase, m$^3$/s; $c_s$ is the particle concentration in the source or sink, mol/m$^3$.

2.2.4 Particle/$CO_2$/oil/water multiphase flow model

The control equation of $CO_2$/oil/water multiphase flow is expressed as

$k_{rj}$ is the relative permeability of the j-th phase; $\mu_j$ is the viscosity of the j-th phase, Pa•s; $q_i$ is the source or sink of the i-th component, mol/s. Besides, the volume of all phases should satisfy

$$V_r\phi\left(1 - \sum_{j=1}^{j=n_p}\frac{n_j\rho_t}{\rho_j}\right) = 0 \quad j = o,g,w, \tag{34}$$

where $\rho_t$ is the total concentration of all components, mol/m$^3$. Eqs. (32)-(34) are the mathematical model of particle/$CO_2$/oil/water multiphase flow.

2.2.5 Particle/$CO_2$/oil/water multiphase flow model

As shown in Fig. 2, taking pressure, component concentration, particle concentration as indispensable variables, the mathematical model of the particle/$CO_2$/crude Oil/aqueous multiphase flow is discretized using the finite volume method and implicit temporal difference. The Collins method is utilized to calculate the partial derivatives of the phase properties, while the partial derivatives of the porosity and permeability are obtained by an automated differentiation method. Thereafter, the Jacobian matrix is assembled, and a linear solver solves the linear equation system. The derived parameters are used to update the phase and rock properties based on the

particle blockage and phase mass transfer models. The above-described simulation method is implemented on the GEOS platform(Gross, 2021).

## 3. RESULTS

### 3.1 Model Validation

As shown in Fig. 3, the core with dimensions of 2.507×2.507×5.152 centimeters is divided into 10 grids (Fig. 3a), and the grid size is 2.507×2.507×0.5152 centimeters. The pore structure parameters obtained from mercury intrusion experiments are listed in Table 1. Based on particle expansion experiments, the parameters for Eq. (29) are shown in Table 2. The composition of the fluid is shown in Table 3. As shown in Table 4, the initial pressure of each grid is set to 8.75 MPa, and the porosity and permeability are 0.14 and 8.7mD. During the injection process, first, $CO_2$ is injected at a flow rate of 0.3 ml/min for 5000 s; then, the particle solution is injected at a flow rate of 0.3 ml/min for 3000 s (Fig. 3b). As shown in Fig. 4, the results of the $CO_2$-responsive particle core displacement experiment indicate that after $CO_2$ flooding, when the particles are injected, the injection pressure increases significantly, demonstrating that the $CO_2$-responsive particles expand upon encountering $CO_2$, and proving the $CO_2$-responsive property of this profile control material. The variation law of the inlet pressure with time obtained from numerical simulation is consistent with the results obtained from core displacement, verifying the correctness of the simulation method for the $CO_2$-responsive particle flow regulation process proposed in this paper.

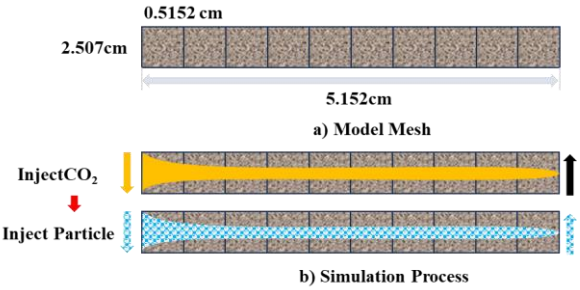


Fig. 3. Numerical simulation for the injection of $CO_2$ - responsive particles into the core

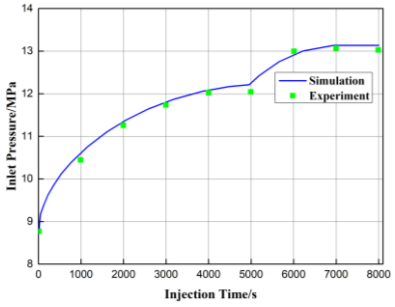


Fig. 4. Comparison between Core Displacement Experiment Results and Simulation Experiment Results

Table 1
Pore structure parameters

| $\eta_1$ | $\lambda_1$ | $\tau_1$ | $\eta_2$ | $\lambda_2$ | $\tau_2$ |
|---|---|---|---|---|---|
| 0.7011 | 378 | 2.757 | 0.2989 | 107.6 | 2.227 |

Table 2
The parameters of the particle expansion model

| $\alpha$ | $\beta$ | $\gamma$ | $K_{a1}$ | $r_{s,max}$ |
|---|---|---|---|---|
| 0.7011 | 2.757 | 0.2989 | $4.7\times10^{-7}$ | 378 |

Table 3
Fluid Composition

| $CO_2$ | $CH_4$ | $C_{7+}$ | $H_2O$ |
|---|---|---|---|
| 0.0 | 0.025 | 0.975 | 0.0 |

Table 4
Reservoir Properties

| Initial Pressure MPa | Porosity | Permeability mD |
|---|---|---|
| 8.75 | 0.14 | 8.7 |

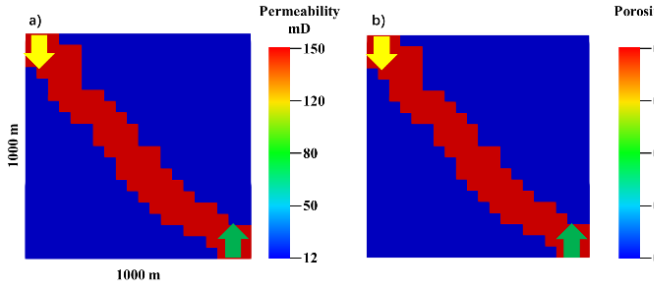


Fig. 5. Reservoir permeability and porosity

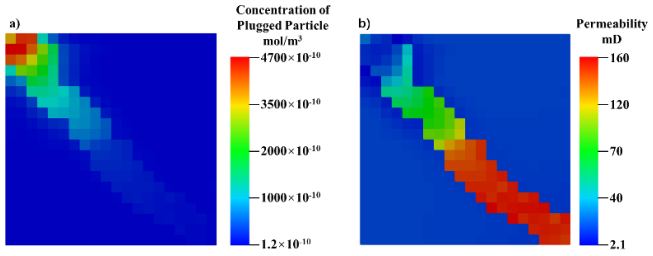


Fig. 6. Particle blockage and its influence on permeability (3652 days)

### 3.2 Simulation Case

A reservoir-scale simulation model is established, with permeability and porosity shown in Fig. 5. The mesh size is 1000 × 1000 × 1 m. The simulation process begins

with a 3-year $CO_2$ injection, followed by a 90-day particle injection, and then concludes with additional $CO_2$ injection. As shown in Fig. 6, the region near the injection well has a high concentration of CO2-responsive particles (Fig. 6a), resulting in a significant decrease in permeability (Fig. 6b). Due to the reduction of horizontal heterogeneity, the $CO_2$ injection flood exhibits a better performance, and the concentration of the C7+ component of the injected particle decreases more than that of the injected no particle (Fig. 7). Based on Fig. 8, the process of particle increases the recovery factor by 7.62%, and enhances the macroscopic sweep factor by 5.52%.

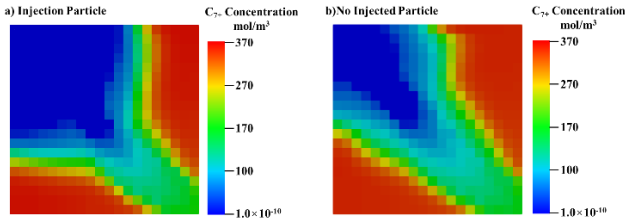


Fig. 7. The distribution of C7+ concentration (3652 day)

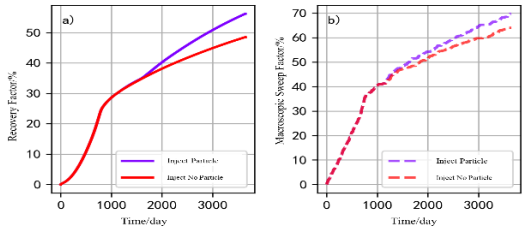


Fig. 8. Comparison between simulation results of inject particle and inject no particle

## *4. DISCUSSION*

In this paper, a new idea is introduced to predict the transport process of $CO_2$-responsive particles, providing new insight into describing particle plugging as a function of particle concentration in a rock. Although this is not straightforward, it can be understood that the particle concentration cannot increase permanently, which results in the concentration of the plugged particles being implicitly constrained.

Moreover, the application of Markov chain theory requires further validation, although the core experiments are well-matched. Specifically, more experiments should be conducted to verify that Eq. (11) is more accurate than Eq. (5).

Finally, this paper gives a simple implication of particle/$CO_2$/oil/water multiphase flow. Some complex problems should be studied in the future, such as the influence of particles on the multiphase relative permeability.

## 5. CONCLUSIONS

In this study, we introduced a novel simulation framework designed to predict the process of $CO_2$ flood enhanced by $CO_2$-responsive particles. The following conclusions are drawn.

1) A straightforward comparison between core displacement experiments and simulations is given to validate the accuracy of the proposed simulation framework for particle/$CO_2$/crude Oil/aqueous multiphase flows. The time-dependent variation of inlet pressure obtained from the simulation is consistent with that from the core displacement experiment.

2) Through the simulation of a field-scale numerical model, the enhancement mechanism of $CO_2$-responsive particles is unveiled. Once the particles are injected, the area near the injection well becomes blocked, resulting in a significant decrease in permeability. Consequently, horizontal heterogeneity is alleviated, which contributes to an increase in macroscopic sweep efficiency and, in turn, enhances the recovery factor. Specifically, in the given cases, the recovery factor increases by 7.62%, and the macroscopic sweep factor increases by 5.52%.


## ACKNOWLEDGEMENT

The authors would like to acknowledge the financial support provided by National Key R&D Program of China (NO. 2022YFE0129900) and National Key R&D Program of China (No. 2019YFA0708700). We are grateful to the financial support provided through National Natural Science Foundation of China (No. 52074338). Bin Yuan would like to thank for the support of National High-Level Young Talent Plan and Shandong Mountain Tai Scholar Program. Wei Zhang wishes to acknowledge the funding from the Shandong Postdoctoral Science Foundation (SDBX2023017).


## DECLARATION OF INTEREST STATEMENT

The authors declare that they have no known competing financial interests or personal relationships that could have appeared to influence the work reported in this paper. All authors read and approved the final manuscript.

## REFERENCE


[1] Abdullah, N., Hasan, N., 2021. Effects of miscible CO2 injection on production recovery. J Petrol Explor Prod

Technol 11, 3543–3557. https://doi.org/10.1007/s13202-021-01223-0
[2] Chen, X., Li, Y., Liu, Z., Zhang, J., Trivedi, J., Li, X., 2023. Experimental and theoretical investigation of the migration and plugging of the particle in porous media based on elastic properties. Fuel 332, 126224. https://doi.org/10.1016/j.fuel.2022.126224
[3] Cheng, L., Tong, M., Luo, J., Liu, R., Sun, G., 2024. In-situ swelling of pH-responsive microgel particles during photopolymerization to mitigate shrinkage stress of UV-cured materials. Reactive and Functional Polymers 195, 105827. https://doi.org/10.1016/j.reactfunctpolym.2024.105827
[4] Deng, J.-N., Zhao, H., Zheng, H., Zhuang, Y., Wei, K., Yuan, H., Deng, Z., Gao, Y., Zhou, X., Yu, T., Hu, H., Lu, G., Zhang, X., 2025. CO2-responsive preformed particle gels with high strength for CO2 conformance control in heterogeneous reservoirs. Fuel 379, 133040. https://doi.org/10.1016/j.fuel.2024.133040
[5] Gross, H., 2021. GEOSX: a multiphysics, multiscale, reservoir simulator for HPC. Presented at the Fifth EAGE Workshop on High Performance Computing for Upstream, European Association of Geoscientists & Engineers, pp. 1–5. https://doi.org/10.3997/2214-4609.2021612014
[6] Guo, H., Lyu, X., Meng, E., Xu, Y., Zhang, M., Fu, H., Zhang, Y., Song, K., 2022. CCUS in China: Challenges and Opportunities. Presented at the SPE Improved Oil Recovery Conference, p. D031S031R002. https://doi.org/10.2118/209468-MS
[7] Liu, Q., Zhao, B., Santamarina, J.C., 2019. Particle Migration and Clogging in Porous Media: A Convergent Flow Microfluidics Study. Journal of Geophysical Research: Solid Earth 124, 9495–9504. https://doi.org/10.1029/2019JB017813
[8] Moghadasi, J., Müller-Steinhagen, H., Jamialahmadi, M., Sharif, A., 2004. Theoretical and experimental study of particle movement and deposition in porous media during water injection. Journal of Petroleum Science and Engineering 43, 163–181. https://doi.org/10.1016/j.petrol.2004.01.005
[9] Sharma, M.M., Yortsos, Y.C., 1987. Transport of particulate suspensions in porous media: Model formulation. AIChE Journal 33, 1636–1643. https://doi.org/10.1002/aic.690331007